Journal of The Electrochemical Society

Electrochemical Properties of $Li_{1+x}CoO_2$ Synthesized for All-Solid-State Lithium Ion Batteries with Li_2S-P_2S_5 Glass-Ceramics Electrolyte

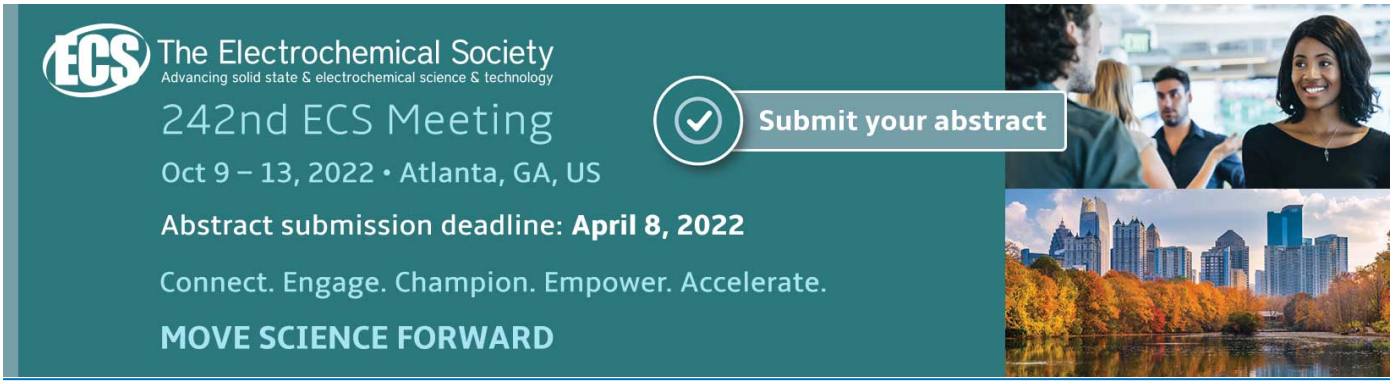

Electrochemical Properties of $Li_{1+x}CoO_2$ Synthesized for All-Solid-State Lithium Ion Batteries with Li_2S-P_2S_5 Glass-Ceramics Electrolyte

Junghoon Kim, Oosup Kim, Chanhwi Park, Giho Lee, and Dongwook Shin[z]

Division of Materials Science & Engineering, Hanyang University, Seongdong-gu, Seoul 133-791, South Korea

The over-stoichiometric $Li_{1+x}CoO_2$ (x = 0.1, 0.2, and 0.3) cathode materials were synthesized from an aqueous solution of lithium nitrate ($LiNO_3$) as an excess lithium precursor and their effects on the electrochemical properties of all-solid-state lithium batteries employing Li_2S-P_2S_5 glass-ceramics solid electrolytes are investigated. A combination of X-ray diffraction, Fourier transform infrared spectroscopy, and inductively coupled plasma atomic emission spectroscopy reveals that the excess lithium forms a residual Li_2CO_3 layer on the surface of as-prepared $Li_{1+x}CoO_2$ particles during the synthesis process. While regarded as an impurity phase in lithium battery systems using liquid electrolytes due to its detrimental effects on electrochemical performance, the Li_2CO_3 formed on the surface of the over-stoichiometric $Li_{1+x}CoO_2$ powders is identified in all-solid-state lithium battery systems using sulfide solid electrolytes to act as an effective coating material to suppress the interfacial side reactions despite its low ionic and electronic conductivity.

 [DOI: 10.1149/2.1051506jes]

Manuscript submitted December 31, 2014; revised manuscript received March 6, 2015. Published March 17, 2015.

All-solid-state lithium ion batteries (ASS-LIBs) including inorganic solid electrolytes are consistently at the center of attention in the discussion on safety issues arising from the flammability of liquid electrolytes in conventional LIBs. ASS-LIB technology has come a long way in the last few decades through the development of oxide and sulfide solid electrolytes with practical levels of high ionic conductivities comparable to organic liquid electrolytes.[1–4] Therefore, the rate determining step is now no longer Li^+ ion migration in the solid electrolyte and overall cell resistance is determined mainly at the interface between the cathode active material and solid electrolyte. However, ASS-LIBs employing oxide and sulfide solid electrolytes have some crucial interfacial problems resulting in low reversible capacity and capacity fade for practical applications, due to limited contact area and undesirable interfacial side reactions between the cathode active material and the oxide/sulfide solid electrolyte.[5,6]

Many studies are in progress to understand and resolve the interfacial side reaction problem responsible for this capacity loss in order to develop ASS-LIBs with high energy density and long cycle life required for electric vehicles. Several researchers have suggested that the origin of the interfacial degradation is mutual diffusion of chemical species between solid electrolyte and cathode,[5,7] or the formation of a space-charge layer.[8,9] When garnet-structured $Li_7La_3Zr_2O_{12}$ (LLZ) is contacted with $LiCoO_2$, mutual diffusion of Co and La, Zr occurs at the interface during a thermal treatment to improve adhesion between the cathode material and the oxide solid electrolyte.[10] Problems regarding this mutual diffusion of Co and S have been also reported in ASS-LIBs with Li_2S-P_2S_5 solid electrolytes, especially during initial charging process. At present, the fundamental mechanism is not clear, but interfacial control via surface modification of oxide cathode powder ($LiMO_2$; M = Mn, Ni, Co) has been generally conducted and proven effective to inhibit this interfacial side reaction and reduce the charge-transfer resistance at the cathode interface in ASS-LIBs involving oxide and sulfide solid electrolytes.[11–15]

Nevertheless, ASS-LIBs are in the pioneering stage, with new frontiers yet to be explored. For instance, while the effects of lithium stoichiometry on transition-metal oxides, which are known as general cathode materials, have been investigated in liquid electrolyte systems,[16–19] none of these studies have been conducted in sulfide solid electrolyte systems yet. The cathode materials studied in ASS-LIBs with sulfide solid electrolytes have been mostly limited to simple lithium transition-metal oxides, such as $LiCoO_2$.

The composition of lithium and transition-metal elements in cathode materials has been reported to influence morphology and surface chemistry, thereby playing a major role in battery performance since charge and mass transfer associated with the electrochemical reaction occur near the surface of cathode materials.[19–21] In addition, it is expected that the influence of these compositions on ASS-LIBs is different from that of the conventional LIBs employing liquid electrolytes. Hence, based on this assumption, we considered it worthy to investigate the effect of lithium stoichiometry on the electrochemical performance of $Li_{1+x}CoO_2$ in sulfide solid electrolyte systems. In this study, we present the synthesis and electrochemical influence of the Li-excess composition $Li_{1+x}CoO_2$ (x = 0.1, 0.2, and 0.3) on the performance of ASS-LIB using Li_2S-P_2S_5 glass-ceramics electrolytes.

Experimental

The $Li_{1+x}CoO_2$ (x = 0.1, 0.2, and 0.3) samples were synthesized from starting materials of reagent grade $LiNO_3$ (98% purity, Junsei) and $Co(NO_3)_2 \cdot 6H_2O$ (98% purity, Sigma-Aldrich). Lithium and cobalt nitrates were dissolved and stirred in deionized water at molar ratios of Li/Co = 1.1, 1.2, and 1.3. Thoroughly mixed nitrate solutions of lithium and cobalt were heated under constant stirring at 80°C until the mixture changed into a sol. The sol was then heated at 150°C until dry. The dried powders were collected and ground by agate mortar and pestle. Subsequently, the as-prepared powders were calcinated at 800°C for 8 h in air to obtain $Li_{1+x}CoO_2$. All experiments were repeated to obtain reproducible synthesis and analysis results of all as-prepared powders.

X-ray diffraction measurements using Cu Kα radiation (λ = 1.54178 Å) were employed to characterize the structure of the calcinated powders (XRD; Ultima IV, Rigaku). XRD data were recorded in the range of 2θ = 15°–70°. Fourier transform infrared (FTIR) spectra were obtained with a FTIR spectrometer (FT-IR; IRAffinity-1, Shimadzu) in the spectral range from 400 to 4000 cm^{-1} with a resolution of 2 cm^{-1}. The sample consisted of pellets prepared by pressing a mechanically homogenized mixture of the as-prepared $Li_{1+x}CoO_2$ powders with dehydrated KBr. The actual Li/Co molar ratios of the $Li_{1+x}CoO_2$ powders were obtained from average values of five parallel experiments by inductively coupled plasma atomic emission spectroscopy (ICP-AES; OPTIMA 4300 DV, Perkin-Elmer).

The morphology of $Li_{1+x}CoO_2$ was analyzed by a scanning electron microscope (SEM; JCM-5700, JEOL).

[z]E-mail: dwshin@hanyang.ac.kr

The electrochemical properties of all $Li_{1+x}CoO_2$ powders in ASS-LIB using Li_2S-P_2S_5 glass-ceramics electrolytes were evaluated by constructing laboratory-scale ASS cells assembled in a CR2032-type coin cell. The composite cathodes as a working electrode were prepared by mixing 39 wt% $Li_{1+x}CoO_2$, 59 wt% $78Li_2S \cdot 22P_2S_5$ glass-ceramics electrolytes, and 2 wt% Super P carbon. The $78Li_2S \cdot 22P_2S_5$ glass-ceramics used as the solid electrolyte was synthesized by high-energy mechanical milling and subsequent heat-treatment.[22] The starting materials of reagent-grade Li_2S (99.9% purity, Alfa Aesar) and P_2S_5 (99% purity, Sigma-Aldrich) were mixed thoroughly in the appropriate molar ratios, and then mechanical milling was performed at 520 rpm for 20 h using a high-energy planetary ball mill (Pulverisette 7, Fritsch). The glass-ceramics was prepared from the milled glass by heat-treatment at 230°C for 3 h in a dry Ar atmosphere. The all-solid-state cells were prepared by sequentially stacking and pressing the composite cathode, solid electrolyte powder, and the indium foil at 290 MPa into a 16-mm-diameter pellet. All cells were charged and discharged in galvanostatic mode at room temperature using a charge-discharge measurement device (TOSCAT-3100, Toyo system). The charge-discharge performance was evaluated under a constant current density of 0.05 C (7.25 mA g^{-1}) and at cut off voltages of 1.9 and 3.68 V (vs. Li-In). The electrochemical impedance spectroscopy measurements of the cells were performed in the frequency range between 0.3 MHz and 0.01 Hz using an impedance analyzer (Solartron 1260) after charging to 3.68 V at 0.05 C.

Results and Discussion

The XRD patterns of the as-prepared $Li_{1+x}CoO_2$ (x = 0.1, 0.2, and 0.3) powders with different lithium stoichiometries are shown in Fig. 1. It is observed that all the patterns exhibited clear splitting of the (006)/(102) and (108)/(110) peaks, indicating that a hexagonal layered structure (α-$NaFeO_2$) with a space group R-3m was formed, in which the oxygen sub-lattice is distorted from a close packed FCC lattice in the direction of the hexagonal c axis.[23,24] This structure has Li ions at the 3a sites and transition metal ions (M = Mn, Co, Ni) at the 3b sites. It is well known that cation mixing caused by partial exchange of Li and Co ions between 3a and 3b sites could give rise to structural disorder. The degree of cation ordering can be identified by the relative integrated intensity ratio (RIR) of the (003) peak to the (104) peak, and the intensity ratio of the hexagonal characteristic doublet peaks (006) and (102) relative to the (101) peak (R factor) in the XRD patterns.[21,23–25] Low RIR and high R factor values mean that cation ordering is reduced. Moreover, when the RIR is below 1.2, either the (006)/(102) peaks or the (108)/(110) peaks become difficult to distinguish from each other. As shown in Table I, all of

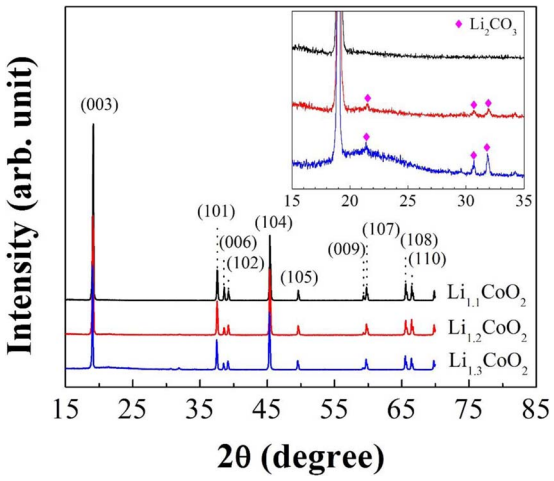

Figure 1. X-ray diffraction (XRD) patterns of the as-prepared $Li_{1+x}CoO_2$ (x = 0.1, 0.2, and 0.3) powders with different lithium stoichiometries.

Table I. Relative integrated intensity ratios (RIR) and R factors of the as-prepared $Li_{1+x}CoO_2$ powders (x = 0.1, 0.2, and 0.3).

Starting composition	RIR $I_{(003)}/I_{(104)}$	R factor $[I_{(006)} + I_{(102)}]/I_{(101)}$
$Li_{1.1}CoO_2$	2.42	0.65
$Li_{1.2}CoO_2$	1.70	0.53
$Li_{1.3}CoO_2$	1.43	0.47

the as-prepared $Li_{1+x}CoO_2$ powders exhibited a high RIR value of above 1.4 and low R factor value of below 0.7, suggesting that all as-prepared $Li_{1+x}CoO_2$ powders have a hexagonal layered structure with an ordered distribution of Li and Co ions in the lattice.

One noticeable feature in the XRD patterns is that residual Li_2CO_3 was observed in the as-prepared $Li_{1.2}CoO_2$ and $Li_{1.3}CoO_2$ powders. Moreover, the intensity of peaks assigned to the Li_2CO_3 phase increased with the amount of excess lithium. It has been reported that over-stoichiometric $Li_{1+x}CoO_2$ synthesized from excess lithium precursor of lithium carbonate (Li_2CO_3) formed residual Li_2CO_3 on the surface during the synthesis process.[26,27] Similar phenomena were observed in this study, although a different synthesis process based on an aqueous solution of lithium nitrate ($LiNO_3$) as an excess lithium precursor was applied to prepare the over-stoichiometric $Li_{1+x}CoO_2$ powders.

The actual Li/Co molar ratios of the as-prepared $Li_{1+x}CoO_2$ powders determined from the ICP values are shown in Table II. From the ICP-AES analysis results, although the loss of lithium was observed during synthesis, all as-prepared $Li_{1+x}CoO_2$ powders showed lithium excess composition after synthesis and the Li/Co molar ratio increased with the amount of excess lithium. The Li/Co molar ratios of the $Li_{1+x}CoO_2$ powders washed by deionized water and the dissolved lithium contents calculated from the difference of Li/Co molar ratio before and after washing of the as-prepared $Li_{1+x}CoO_2$ are also included in Table I to verify the existence of surface Li_2CO_3. After washing, the Li/Co molar ratios of all $Li_{1+x}CoO_2$ powders decreased to ~1 and the dissolved lithium contents from the as-prepared $Li_{1+x}CoO_2$ increased with the amount of excess lithium, suggesting that a larger amount of water soluble Li_2CO_3 was removed from the surface of the as-prepared $Li_{1+x}CoO_2$. A notable feature is that the Li/Co molar ratio of as-prepared $Li_{1+x}CoO_2$ (x = 0.2 and 0.3) powders converged to 1.06 after washing. It has been reported that a small amount of excess lithium in the over-stoichiometric $Li_{1+x}CoO_2$ forms a $Li_{1+x}Co_{1-x}O_{2-\delta}$ phase with a solid solution limit of Li/Co = 1.15 within the bulk material and most of the excess lithium forms Li_2CO_3 on the surface of $Li_{1+x}Co_{1-x}O_{2-\delta}$ phase.[16,17,27] All findings suggest that the as-prepared $Li_{1+x}CoO_2$ powders (x = 0.1, 0.2, and 0.3) consist of an inner Li excess $Li_{1+x}CoO_2$ particle with a solid solution limit of Li/Co = 1.06 and outer surface layer of residual Li_2CO_3. However, the inner particles of $Li_{1+x}CoO_2$ exhibit a lower solid solution limit than the reported value, which is probably due to different reaction mechanisms or synthesis method, different starting materials used as lithium and cobalt sources, and calcination temperature.

To further confirm the existence of residual Li_2CO_3 on the surface of as-prepared $Li_{1+x}CoO_2$ particles, FT-IR analysis results are shown

Table II. Actual Li/Co molar ratios determined by ICP-AES for the as-prepared $Li_{1+x}CoO_2$ powders before and after washing by deionized water.

Starting ratio	ICP values (Actual Li/Co molar ratios)		Dissolved Li content Mole of Li
	As-prepared powders	Washed powders	
1.1	1.0578 (1.06)	1.0045 (1.00)	0.0077
1.2	1.1438 (1.14)	1.0628 (1.06)	0.0117
1.3	1.2075 (1.21)	1.0566 (1.06)	0.0217

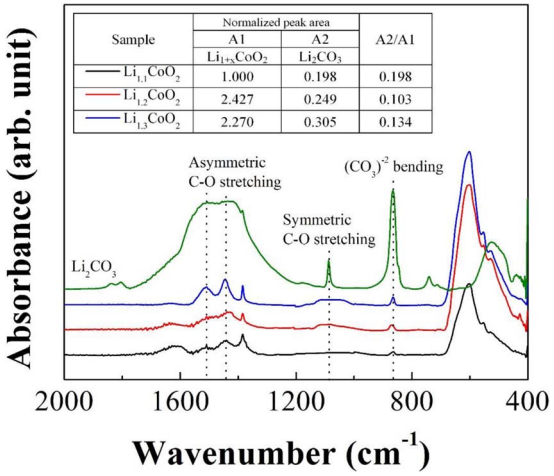

Figure 2. Fourier transform infrared (FTIR) spectra of the as-prepared $Li_{1+x}CoO_2$ (x = 0.1, 0.2, and 0.3) powders with different lithium stoichiometries.

in Fig. 2. All as-prepared $Li_{1+x}CoO_2$ powders showed similar absorption peak at around 600 cm^{-1} originated from $LiCoO_2$ phase,[28] which explains successful synthesis of layered $LiCoO_2$ structure. However, as shown by the reference spectrum of Li_2CO_3, the absorption peaks of Li_2CO_3 associated with vibrational modes of the carbonate ions were observed in the FT-IR spectra of all as-prepared $Li_{1+x}CoO_2$ powders and the intensity of absorption peaks increased with the amount of excess lithium.[29] Moreover, the relative area ratio (A2/A1) of the peaks associated with vibrational modes of the carbonate ions to the peaks originated from the lithium cobalt oxide increased as the amount of excess lithium increased from 1.2 to 1.3, although it was difficult for the as-prepared $Li_{1.1}CoO_2$ powder with the smaller Li/Co molar ratio of the inner Li excess $Li_{1+x}CoO_2$ particle (1.00) to be directly compared due to too low intensity of the peaks originated from the lithium cobalt oxide resulting in the high relative area ratio (A2/A1). These results supports the presence of residual Li_2CO_3 on the surface of as-prepared $Li_{1+x}CoO_2$ particles.

In Fig. 3, the SEM images show that the as-prepared $Li_{1+x}CoO_2$ powders consist of irregular particles with rounded edges and largely agglomerated primary particles of a few micrometers size. The evident difference in the morphology is that the amount of Li_2CO_3 covering the surface of $Li_{1.2}CoO_2$ and $Li_{1.3}CoO_2$ particles remarkably increased compared with the $Li_{1.1}CoO_2$ particles showing partially smooth and clean surface. From the ICP and SEM results, it is considered that the amount of Li_2CO_3 covering the surface of $Li_{1+x}CoO_2$ particle gradually increased as the amount of excess lithium increased. In addition, the SEM images of the as-prepared $Li_{1.2}CoO_2$ and $Li_{1.3}CoO_2$ powders washed by deionized water, shown in Fig. 4, provide a direct evidence of surface Li_2CO_3. Compared with the as-prepared $Li_{1.2}CoO_2$ and $Li_{1.3}CoO_2$ powders without washing, a markedly clearer and smoother surface was observed in the washed $Li_{1.2}CoO_2$ and $Li_{1.3}CoO_2$ powders, which suggests the surface Li_2CO_3 had been rinsed away.

Fig. 5a shows the first charge and discharge curves of ASS-LIBs using the as-prepared $Li_{1.2}CoO_2$ and washed $Li_{1.2}CoO_2$ powders. An interesting feature is that the as-prepared $Li_{1.2}CoO_2$ powder with Li_2CO_3 on the surface of inner $Li_{1.06}CoO_2$ particles exhibited stable charge and discharge properties without significant polarization, while the washed $Li_{1.2}CoO_2$ powders having clear surface exhibited a rapid increase of voltage during the initial charging step. The similar phenomena were also observed for washing of the as-prepared $Li_{1.1}CoO_2$ and $Li_{1.3}CoO_2$ powders. Although there is difference in the amount of Li_2CO_3, novel feature is that all Li_2CO_3 coated $Li_{1+x}CoO_2$ powders exhibited normal charge-discharge behavior whereas all Li_2CO_3 free $Li_{1+x}CoO_2$ powders didn't.

This severe degradation of charge-discharge properties of the washed $Li_{1+x}CoO_2$ powders can be explained by electrochemical

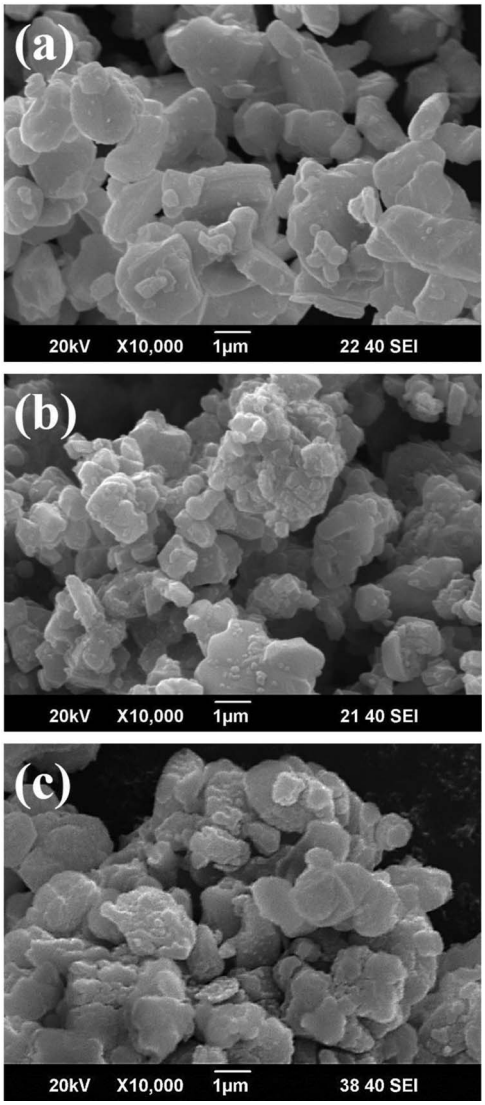

Figure 3. Scanning electron microscope (SEM) images of the as-prepared (a) $Li_{1.1}CoO_2$, (b) $Li_{1.2}CoO_2$, and (c) $Li_{1.3}CoO_2$ powders.

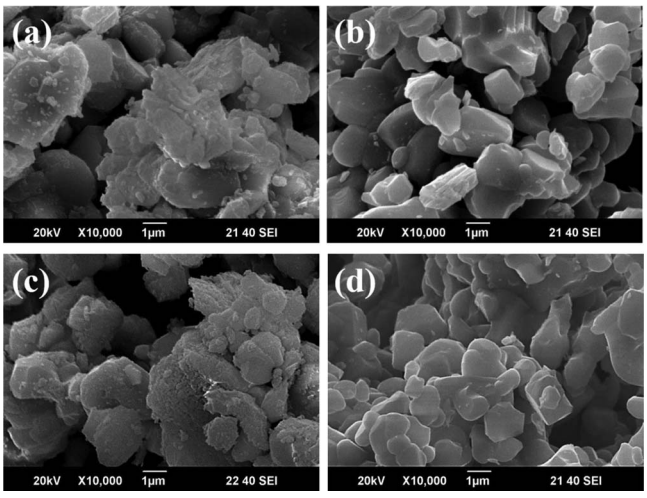

Figure 4. Scanning electron microscope (SEM) images of the (a) as-prepared $Li_{1.2}CoO_2$ powder, (b) washed $Li_{1.2}CoO_2$ powder, (c) as-prepared $Li_{1.3}CoO_2$ powder and (d) washed $Li_{1.3}CoO_2$ powder.

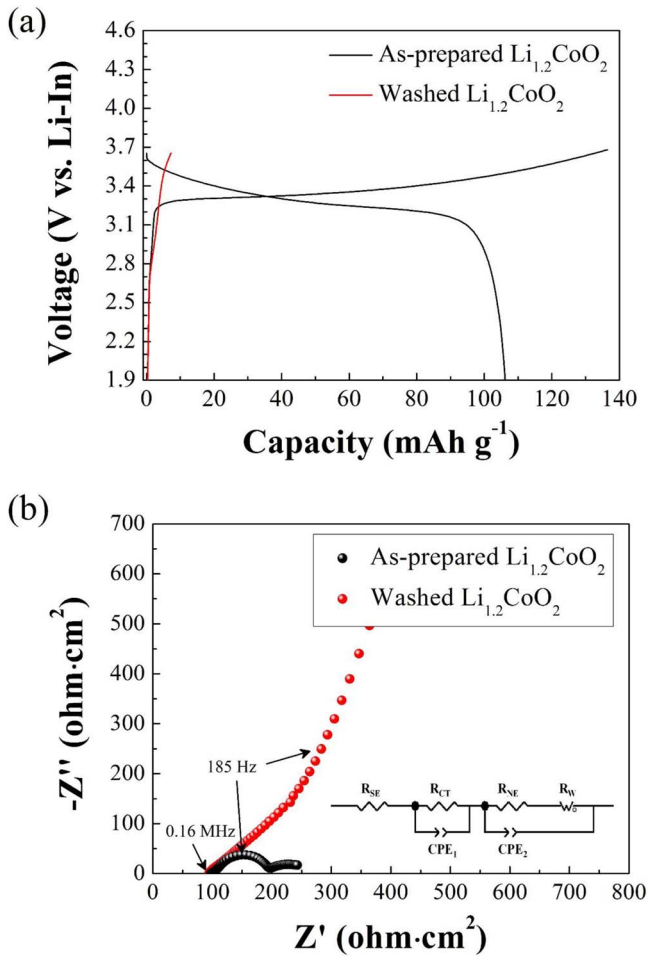

Figure 5. (a) Galvanostatic initial charge/discharge profiles and (b) AC impedance spectra for all-solid-state lithium batteries using the as-prepared $Li_{1.2}CoO_2$ and washed $Li_{1.2}CoO_2$ powders.

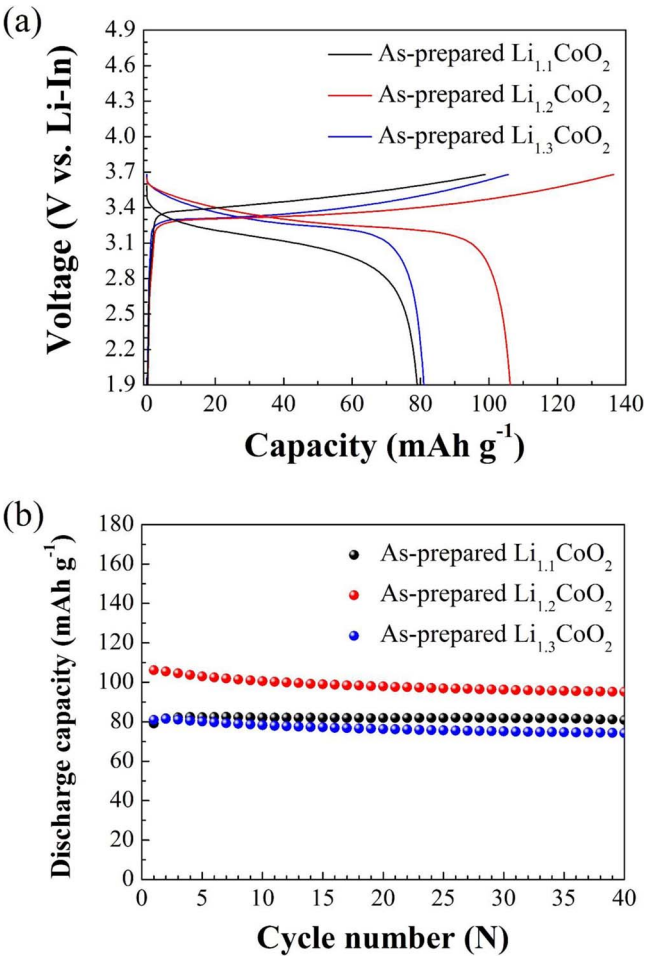

Figure 6. (a) Galvanostatic initial charge/discharge profiles and (b) discharge capacity as a function of cycle number for all-solid-state lithium batteries using the as-prepared $Li_{1+x}CoO_2$ (x = 0.1, 0.2, and 0.3) powders with different lithium stoichiometries.

impedance results of Fig. 5b. The AC impedance spectra of ASS-LIB using the as-prepared $Li_{1+x}CoO_2$ powders consisted of three resistance components at high (R_{SE}), medium (R_{CT}), and low (R_{NE}) frequency. The R_{SE} at the high frequency region is identified as the resistance of solid electrolytes. The R_{NE} at the low frequency region is identified as the resistance of the indium negative electrode related to diffusion of lithium ions in the indium electrode, which is affected by changes in lithium ion concentration according to the charging state of the cells.[30] In addition, the R_{CT} at medium frequency is attributed to the charge-transfer resistance at the interface between cathode materials and solid electrolytes in composite cathodes, which is greatly affected by interfacial reactions and reduced by coating processes. Excessively large charge-transfer resistance (R_{CT}) of the washed $Li_{1.2}CoO_2$ particles indicates that the fresh and clear surface of that was unprotected from the interfacial reaction, while the inherent interfacial reaction between oxide cathode materials and sulfide solid electrolytes was greatly suppressed by Li_2CO_3 on the surface of the as-prepared $Li_{1.2}CoO_2$ particles.

In conventional LIBs with liquid electrolytes, it has been generally reported that the presence of Li_2CO_3 produces harmful results such as accelerated gas formation by catalyzed electrolyte decomposition, which is one of the main sources of cell swelling at high temperature,[31,32] and reduction of interfacial kinetics due to its low ionic and electronic conductivity at room temperature.[27] Both result in lower reversible capacity and rapid capacity fade. In addition, it has been reported that the Li_2CO_3 layer results in the large charge-transfer resistance at the interface between the surface of oxide solid electrolyte such as LLZO and the lithium metal anode.[33] Therefore, it is common to remove Li_2CO_3 from the surface of cathode and solid electrolyte material by post treatments such as heating, washing and polishing.[32–34] However, in this study, it is observed in the ASS-LIB system using sulfide solid electrolytes that the Li_2CO_3 acts as an effective coating material rather than an impurity phase, which results in suppression of the interfacial reaction by formation of a physical barrier.

Considering the effect and amount of residual Li_2CO_3, it could be speculated that the as-prepared $Li_{1.3}CoO_2$ powder might show the highest reversible capacity and the as-prepared $Li_{1.1}CoO_2$ powder the lowest reversible capacity. However, in Figs. 6a and 6b, the as-prepared $Li_{1.2}CoO_2$ powder exhibited the highest initial charge and discharge capacities of 136 and 106 mAh g^{-1}, respectively. The lower reversible capacity of the as-prepared $Li_{1.3}CoO_2$ powders in all cycles, as well as initial cycle, is due to slower interfacial kinetics dictated by excess Li_2CO_3 content at the surface despite the as-prepared $Li_{1.2}CoO_2$ and $Li_{1.3}CoO_2$ powders consisting of inner particles with a similar Li/Co molar ratio of 1.06. On the other hand, the reason for better charge and discharge performance of the as-prepared $Li_{1.2}CoO_2$ powder compared with the as-prepared $Li_{1.1}CoO_2$ powder is a combined result of surface coating and lithium doping. Firstly, the amount of Li_2CO_3 covering the inner particle of as-prepared $Li_{1.1}CoO_2$ was insufficient to suppress the undesirable interfacial reaction, which increased internal resistance of cell during initial charging resulting in decrease of discharge voltage. In addition, the inner particle of as-prepared $Li_{1.2}CoO_2$ showed an over-stoichiometric composition and

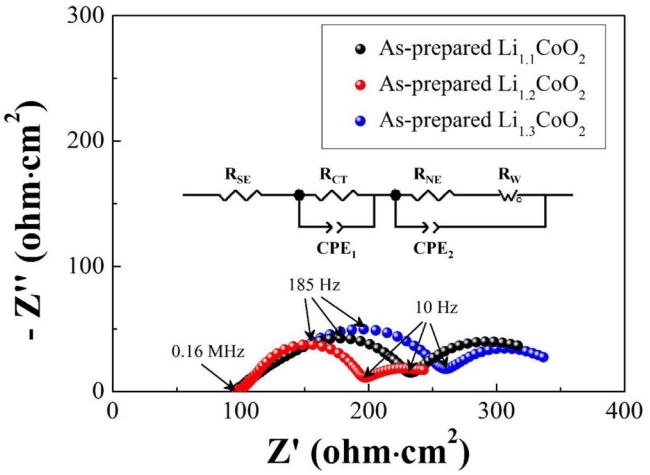

Figure 7. AC impedance spectra of all-solid-state lithium batteries using the as-prepared $Li_{1+x}CoO_2$ (x = 0.1, 0.2, and 0.3) powders with different lithium stoichiometries.

the unfavorable phase transition associated with the monoclinic distortion of the O3 hexagonal phase over 3.58 V vs. Li-In (4.2 V vs. Li/Li^+) did not occur.[16,17]

The superior performance of the as-prepared $Li_{1.2}CoO_2$ powder is further supported by electrochemical impedance results compared in Fig. 7. The AC impedance profile of ASS-LIB using the as-prepared $Li_{1.2}CoO_2$ powder showed the lowest charge-transfer resistance (R_{CT}), indicating that the Li_2CO_3 covering the surface of as-prepared $Li_{1.2}CoO_2$ powder remarkably suppressed the interfacial reaction which hinders the intercalation/deintercalation process of Li ions. In addition, the highest charge capacity of that enhanced lithium ion concentration in the indium electrode, which resulted in the lowest resistance of the indium negative electrode (R_{NE}).

Although detailed studies on the bulk crystallographic properties of the as-prepared $Li_{1+x}CoO_2$ powders, such as the oxidation state of the Co ions and oxygen defects, are needed to provide more information about the relationship with electrochemical performance of ASS-LIBs involving sulfide solid electrolytes, it is shown in this study that the surface Li_2CO_3 acts as a physical barrier to effectively reduce the charge-transfer resistance of the ASS-LIBs involving sulfide solid electrolytes despite low ionic and electronic conductivity, which results in the enhancement of cycle performance. We believe that the data here reported, even if still at a preliminary stage, are of importance for the progress of the ASS-LIBs using sulfide solid electrolytes. In addition, the future work to optimize the amount of Li_2CO_3 on the surface of $LiCoO_2$ is in progress.

Conclusions

Li_2CO_3 coated over-stoichiometric $Li_{1+x}CoO_2$ powders with a solid solution limit of Li/Co = 1.06 were synthesized from lithium and cobalt nitrate sources with a nominal ratio of Li/Co > 1. The as-prepared $Li_{1.2}CoO_2$ powders with an actual Li/Co molar ratio of 1.14 exhibited the highest charge and discharge capacities of 136 and 106 mAh g^{-1}, respectively, demonstrating that the small amount of Li_2CO_3 on the surface of cathode materials exhibited a beneficial effect on the interfacial properties leading to improved charge and discharge performance of ASS-LIBs using sulfide solid electrolytes. Exploration and application of coating materials for ASS-LIBs using sulfide solid electrolytes is a critical issue to reduce inherently high charge-transfer resistance induced by interfacial side reaction between oxide cathode materials and sulfide solid electrolytes. In this sense, these results are convincing in demonstrating that the Li_2CO_3 naturally formed on the surface by simply adjusting the composition of starting materials is a cost-effective and useful coating material to suppress the interfacial side reaction of cathode materials with sulfide solid electrolytes in ASS-LIBs.

Acknowledgments

This work is supported by the National Strategic R&D Program for Industrial Technology (10043868), funded by the Ministry of Trade, Industry, and Energy (MOTIE).

References

1. N. Kamaya, K. Homma, Y. Yamakawa, M. Hirayama, R. Kanno, M. Yonemura, T. Kamiyama, Y. Kato, S. Hama, K. Kawamoto, and A. Mitsui, *Nat. Mater.*, **10**, 682 (2011).
2. S. Ujiie, A. Hayashi, and M. Tatsumisago, *J. Solid State Electrochem.*, **17**, 675 (2012).
3. Y. Seino, T. Ota, K. Takada, A. Hayashi, and M. Tatsumisago, *Energy & Environmental Science*, **7**, 627 (2014).
4. R. Murugan, V. Thangadurai, and W. Weppner, *Angew. Chem. Int. Ed.*, **46**, 7778 (2007).
5. A. Sakuda, A. Hayashi, and M. Tatsumisago, *Chem. Mater.*, **22**, 949 (2010).
6. H. Kitaura, A. Hayashi, T. Ohtomo, S. Hama, and M. Tatsumisago, *J. Mater. Chem.*, **21**, 118 (2011).
7. J. H. Woo, J. E. Trevey, A. S. Cavanagh, Y. S. Choi, S. C. Kim, S. M. George, K. H. Oh, and S. H. Lee, *J. Electrochem. Soc.*, **159**, A1120 (2012).
8. N. Ohta, K. Takada, L. Zhang, R. Ma, M. Osada, and T. Sasaki, *Adv. Mater.*, **18**, 2226 (2006).
9. J. Haruyama, K. Sodeyama, L. Han, K. Takada, and Y. Tateyama, *Chem. Mater.*, **26**, 4248 (2014).
10. K. H. Kim, Y. Iriyama, K. Yamamoto, S. Kumazaki, T. Asaka, K. Tanabe, C. A. Fisher, T. Hirayama, R. Murugan, and Z. Ogumi, *J. Power Sources*, **196**, 764 (2011).
11. N. Ohta, K. Takada, I. Sakaguchi, L. Zhang, R. Ma, K. Fukuda, M. Osada, and T. Sasaki, *Electrochem. Commun.*, **9**, 1486 (2007).
12. A. Sakuda, H. Kitaura, A. Hayashi, K. Tadanaga, and M. Tatsumisago, *J. Power Sources*, **189**, 527 (2009).
13. Y. Seino, T. Ota, and K. Takada, *J. Power Sources*, **196**, 6488 (2011).
14. K. Okada, N. Machida, M. Naito, T. Shigematsu, S. Ito, S. Fujiki, M. Nakano, and Y. Aihara, *Solid State Ionics*, **255**, 120 (2014).
15. S. Ito, S. Fujiki, T. Yamada, Y. Aihara, Y. Park, T. Y. Kim, S. Baek, J. Lee, S. Doo, and N. Machida, *J. Power Sources*, **248**, 943 (2014).
16. N. Imanishi, M. Fujii, A. Hirano, Y. Takeda, M. Inaba, and Z. Ogumi, *Solid State Ionics*, **140**, 45 (2001).
17. N. Imanishi, M. Fujii, A. Hirano, and Y. Takeda, *J. Power Sources*, **97–98**, 287 (2001).
18. E. Antolini, *Solid State Ionics*, **170**, 159 (2004).
19. M. Zou, M. Yoshio, S. Gopukumar, and J. Yamaki, *Mater. Res. Bull.*, **40**, 708 (2005).
20. M. Zou, M. Yoshio, S. Gopukumar, and J. Yamaki, *Chem. Mater.*, **15**, 4699 (2003).
21. K. Elong, N. Kamarulzaman, R. Rusdi, N. Badar, and M. H. Jaafar, *ISRN Condensed Matter Physics*, **2013**, 1 (2013).
22. J. Kim, M. Eom, S. Noh, and D. Shin, *J. Power Sources*, **244**, 476 (2013).
23. Y. Gao, M. V. Yakovleva, and W. B. Ebner, *Electrochem. Solid-State Lett.*, **1**, 117 (1998).
24. J. Cho, G. Kim, and H. S. Lim, *J. Electrochem. Soc.*, **146**, 3571 (1999).
25. T. Ohzuku, A. Ueda, M. Nagayama, Y. Iwakoshi, and H. Komori, *Electrochim. Acta*, **38**, 1159 (1993).
26. M. Carewska, S. Scaccia, F. Croce, S. Arumugam, Y. Wang, and S. Greenbaum, *Solid State Ionics*, **93**, 227 (1997).
27. N. Pereira, C. Matthias, K. Bell, F. Badway, I. Plitz, J. Al-Sharab, F. Cosandey, P. Shah, N. Isaacs, and G. G. Amatucci, *J. Electrochem. Soc.*, **152**, A114 (2005).
28. Z. Wang, X. Huang, and L. Chen, *J. Electrochem. Soc.*, **150**, A199 (2003).
29. S. Yamamoto, C. Kawakami, and Y. Mizuyori, *Electrical Engineering in Japan*, **148**, 22 (2004).
30. A. Sakuda, H. Kitaura, A. Hayashi, K. Tadanaga, and M. Tatsumisago, *J. Electrochem. Soc.*, **156**, A27 (2009).
31. A. M. Andersson, D. P. Abraham, R. Haasch, S. MacLaren, J. Liu, and K. Amine, *J. Electrochem. Soc.*, **149**, A1358 (2002).
32. J. Kim, Y. Hong, K. S. Ryu, M. G. Kim, and J. Cho, *Electrochem. Solid-State Lett.*, **9**, A19 (2006).
33. L. Cheng, E. J. Crumlin, W. Chen, R. Qiao, H. Hou, S. Franz Lux, V. Zorba, R. Russo, R. Kostecki, Z. Liu, K. Persson, W. Yang, J. Cabana, T. Richardson, G. Chen, and M. Doeff, *PCCP*, **16**, 18294 (2014).
34. Z. Chen and J. R. Dahn, *Electrochem. Solid-State Lett.*, **7**, A11 (2004).